JOURNAL OF MATERIALS SCIENCE 23 (1988) 3332–3337

Fracture on rubber–metallic cord composites

A. J. MARZOCCA*‡, R. RAGGI*
*FATE SAICI, Grupo de Investigación, Av. Blanco Encalada 3003, San Fernando, Prov. de Buenos Aires (1644), Argentina
‡Universidad de Buenos Aires, Facultad de Ciencias Exactas y Naturales, Departamento de Física, Lab. Polímeros y Materiales Compuestos, Ciudad Universitaria, Pabellón 1, Buenos Aires (1428), Argentina

Fracture mechanisms in rubber–metal cord composites are studied in the fatigue mode. A test method using TCAT specimens is discussed. Results of the composite life, for different levels of cure in fatigue at constant deformation are presented. Data are analysed by an energetic model and with a finite element technique in terms of the crack propagation along the cord.

1. Introduction

In modern radial tyre technology, the steel cord to rubber matrix adhesion strength is a subject of a great interest. Several methods have been proposed to study and evaluate their properties [1–5]. At least in the case of simple test specimens, the test methods usually measure the pullout force. However, it is apparent that the fracture modes do not depend only on the material properties but also on the time dependence of the applied force. In particular, it seems to be of interest to test the fatigue mode, in accordance with the service conditions.

The purpose of this paper is to discuss a test method based upon a simple test specimen (TCAT) [6–8] that allows us to study the relationship between failure modes and material properties in connection with the severity, tearing energy and stress–strain fields intensity.

2. Failure characterization

In the TCAT specimen, the maximum shear stress is located at the ends of the embedded cords [6, 9]. It has been observed that in the pullout test the failure propagates in different ways:

(a) through the cord–rubber adhesion interface (adhesive mode),

(b) through the rubber surrounding the cord (longitudinal cohesive mode),

(c) perpendicular to the cord direction, starting at the end (transverse cohesive mode).

The following theoretical considerations refer to the first two modes.

3. Theory

3.1. The tearing energy for the TCAT test piece

We utilize the Griffith criterion, adapted to elastomeric materials by Rivlin–Thomas [10, 11] for fracture propagation, based on the tearing energy concept, according to which

$$\alpha = -\partial U/\partial S \tag{1}$$

is the critical condition for propagation, where U stands for the total elastic energy of the deformed specimen, S is the area of the free surface generated by the fracture, and α the tearing energy, dependent on specimen geometry, deformation fields and rubber properties.

Fig. 1 shows the geometry and dimensions of the test piece. The deformation definition for the invariant volume that will be utilized is

$$\varepsilon = \ln(1 + e) \tag{2}$$

where $e = \Delta l/(c_0 + c')$, and c_0 is the relaxed distance between cord ends, c' the propagation distance of the crack, and Δl the overall amplitude of the deformation. If $e \ll 1$ then the usual deformation definition constitutes a good approximation. Expression 2 may be rewritten as

$$\varepsilon = \ln\left(1 + \frac{\varepsilon_0}{1 + x}\right) \tag{3}$$

where $\varepsilon_0 = \Delta l/c_0$ and $x = c'/c_0$. The stored elastic energy density is,

$$w = \tfrac{1}{2}E\varepsilon^2 = \tfrac{1}{2}E\left[\ln\left(1 + \frac{\varepsilon_0}{1 + x}\right)\right]^2 \tag{4}$$

where E is Young's modulus. If V represents the volume limited by the sections reached by the debonding process (initially it corresponds to the ends of the wires),

$$V = A(c' + c_0) = Ac_0(1 + x)$$

where A is the transverse area of the relaxed specimen, then

$$U = (V_w/2)w = \frac{EA}{2}c_0(1 + x)\left[\ln\left(1 + \frac{\varepsilon_0}{1 + x}\right)\right] \tag{5}$$

from Equation 1, where $S = \pi Dc'$ is the debonded area and D the wire diameter, we obtain

$$\alpha = \frac{EA}{2\pi D}\left[2\frac{[\varepsilon_0/(1 + x)]}{1 + [\varepsilon_0/(1 + x)]} - \ln\left(1 + \frac{\varepsilon_0}{1 + x}\right)\right] \times \ln\left(1 + \frac{\varepsilon_0}{1 + x}\right) \tag{6}$$

0022–2461/88 $03.00 + .12

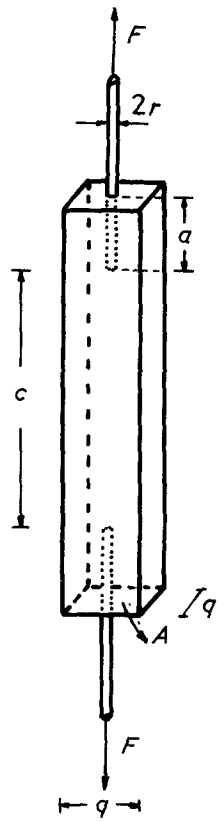

Figure 1 Dimensions of the TCAT test probe. $a = 20\,\text{mm}$, $c = 35\,\text{mm}$, $r = 0.7\,\text{mm}$, $q = 12.5\,\text{mm}$.

and if we consider the limit where $\varepsilon_0/(1 + x) \ll 1$, then

$$\alpha = \frac{EA}{2\pi D}\left(\frac{\varepsilon_0}{1 + x}\right)^2 \tag{7}$$

3.2. Propagation through the rubber matrix

At this point we assume that the debonding process occurs as a cohesive fracture in the rubber matrix in the immediate vicinity of the adhesion interface. In this case, the Griffith criterion for propagation can be applied, and the rate of crack growth, measured as the new fractured area created per cycle, is characteristic for the particular rubber composition. In the range of moderate to high strain it is given by

$$\pi D\, \mathrm{d}c'/\mathrm{d}n = B\alpha^{\beta} \tag{8}$$

where n is the number of cycles and β and B are material constants.

For low strains, a linear relationship of the form

$$\pi D\, \mathrm{d}c'/\mathrm{d}n = K(\alpha - \alpha_0) \tag{9}$$

is applicable where α_0 represents a minimum tearing energy under which there is no propagation and K is a proportionality constant related to the crack propagation rate.

From Equations 7 and 9 we obtain

$$\frac{\mathrm{d}c'}{\mathrm{d}n} = \frac{K}{\pi D}\left(\frac{C^2}{u^2} - \frac{1}{\gamma^2}\right) \tag{10}$$

where $u = 1 + x$, $\gamma = \alpha_0^{-1/2}$ and $C = (EA/2\pi D)^{1/2}\varepsilon_0$. It is possible to integrate Equation 10 in order to obtain the number of cycles to failure, N

$$N = \frac{\pi D c_0 \gamma^2}{K}\left(-\xi + \frac{C\gamma}{2}\frac{(C + 1 + \xi)}{(C - 1 - \xi)}\frac{(C - 1)}{(C + 1)}\right) \tag{11}$$

where $\xi = a/c_0$ has been defined. For the range of higher tearing energies

$$N = \frac{l_0 2^{\beta}(\pi D)^{\beta+1}}{B(EA\varepsilon_0^2)}\left(\frac{1}{2\beta + 1}\right) \times \left(\frac{(1 + \xi)^{2\beta+1} - 1}{1 + 2\xi}\right) \tag{12}$$

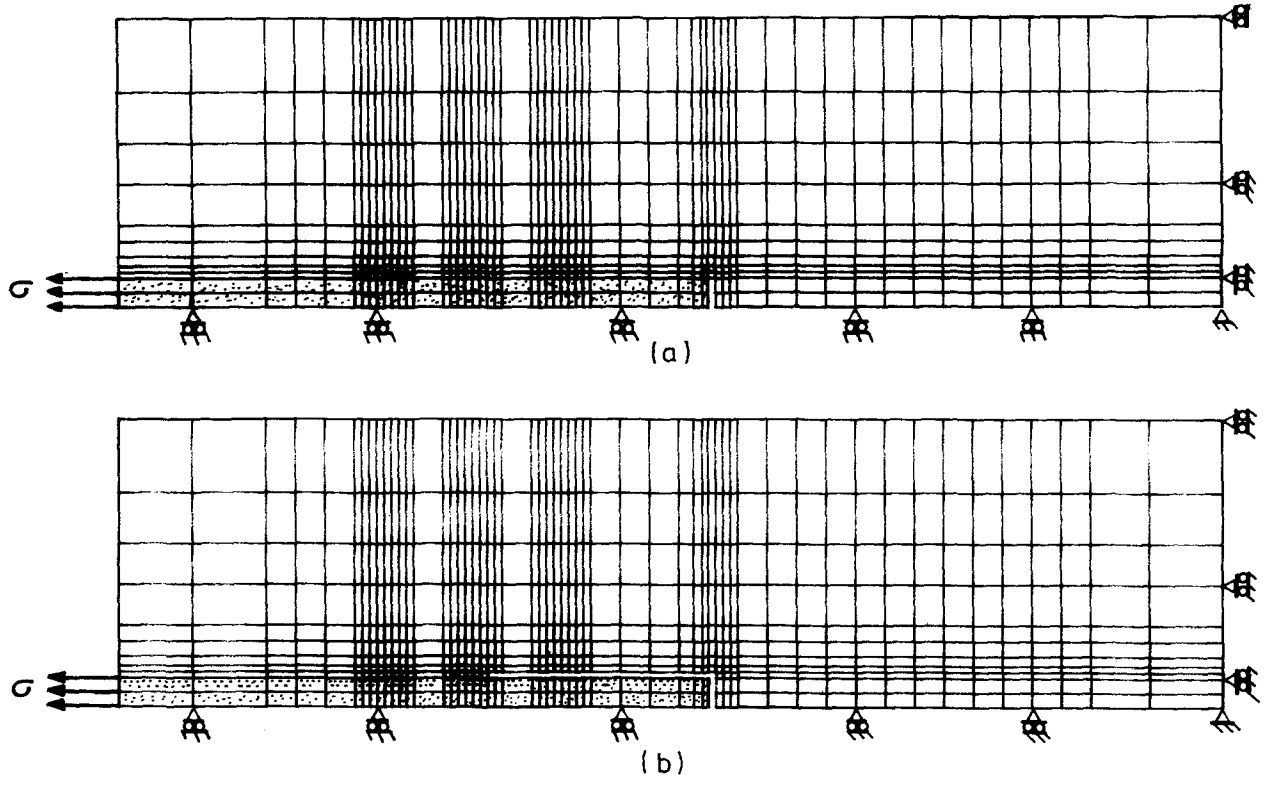

Figure 2 Mesh for finite element calculations. (a) without and (b) with crack propagation.

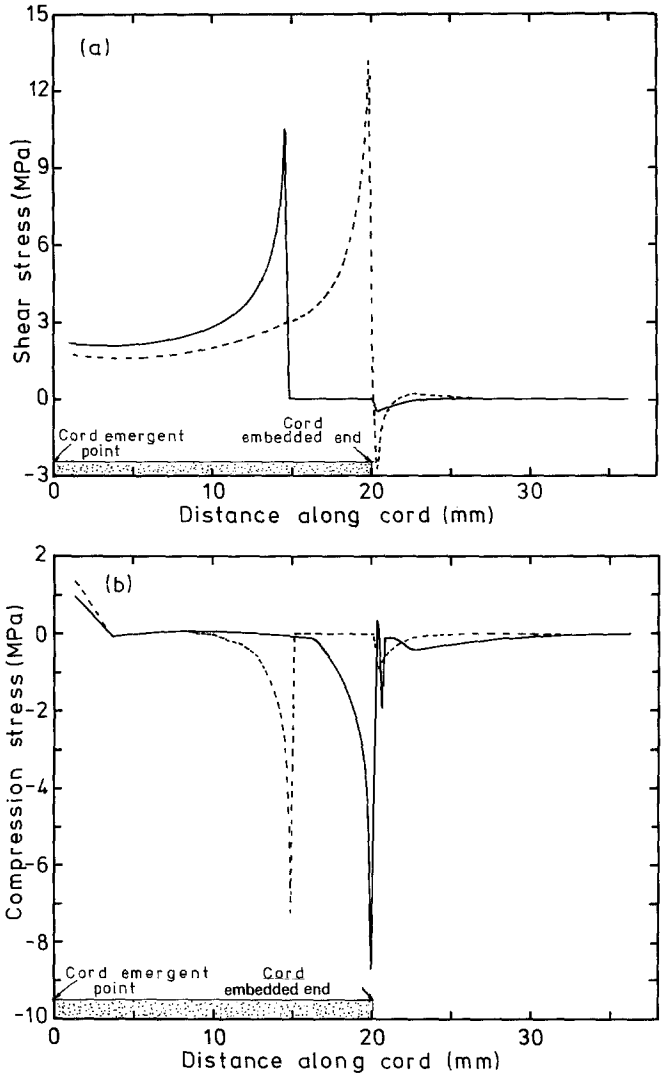

Figure 3 Variation of (a) the shear stress and (b) compression stress over the cord. The dotted lines denote propagation and the full lines when the crack is propagated. E_r = 12.1 MPa, V_A = 0.49, E_c = 152 GPa, V_c = 0.3, Δl = 4 mm.

where $l_0 = c_0 + 2a$ is the total length of the TCAT test piece. During the propagation the tearing energy decreases monotonically due to the increase in the distance $c_0 + c'$. Then, if the condition

$$\frac{EA}{2\pi D}\frac{\varepsilon_0^2}{(1+x)^2} = \alpha_0$$

holds for any point of the fracture path, the growth should stop, at least in the case of slow clamp speed. It is easy to show that the condition for this not to occur is

$$a > c_0[(EA/2\pi D\alpha_0)^{-1/2}\varepsilon_0 - 1] \qquad (13)$$

for a level of deformation ε_0. It is possible to determine the parameters α_0 and K which characterize the fracture material properties under fatigue conditions (small amplitudes) by carrying out independent experiments with different initial tearing energy amplitudes and using Equation 11.

3.3. Stress–strain fields in the TCAT specimen

Ridha *et al.* [9] calculated the strain fields in the TCAT specimen by means of the finite elements method (FEM). With the same approach, results are presented here for the case in which the fracture has propagated a certain distance from the end of the cord.

Taking into account the symmetries of the TCAT specimen and approximating the cross section by a circular one with the same area, the stress–strain fields were calculated for the quadrant shown in the mesh of Fig. 2, with axial symmetry. Figs 3a and b show the shear and compression stress distribution along the cord when the fracture has propagated a given distance.

Fig. 4 shows the peak shear strain (at the front of the fracture) as a function of that distance. From a consideration of the small region where the compression stress has values significantly different from zero, an estimation of the energy lost by friction in a deformation cycle shows that this is negligible compared with the dissipation in the bulk of the material. This fact allows us to apply, without corrections, the Rivlin–Thomas [10] approach to the fracture analysis, based upon the Griffith criterion, to the TCAT test piece under cyclic tensile deformation.

4. Experimental results

TCAT test specimens were prepared with a compound whose basic components are given in Table I. It used a multifilament wire (construction 3 + 9 + 15 × 0.22 + 1 × 0.15) of 1.4 mm in diameter and an embedded length of 18 mm. They were vulcanized in three groups under different temperatures, with a 100% degree of cure, according to Table II. The tests

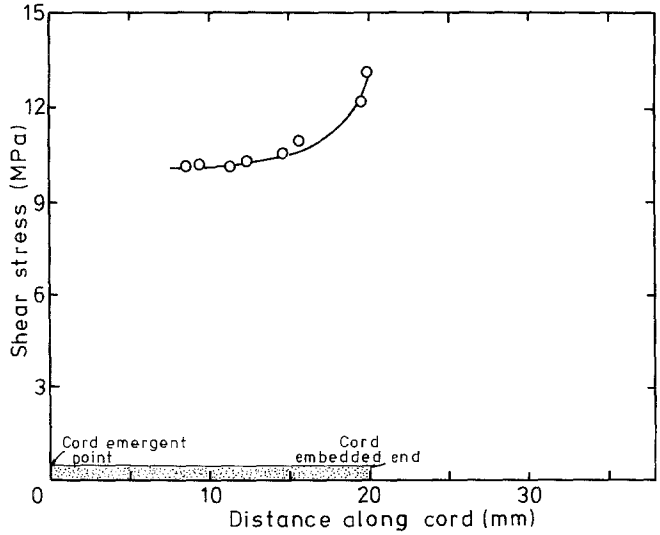

Figure 4 Variation of the maximum shear stress when the crack is propagated along the cord. E_r = 12.1 MPa, V_r = 0.49, E_c = 152 GPa, V_c = 0.3, Δl = 4 mm.

were performed in a DeMattia fatigue tester at a frequency of 5.5 Hz at 40° C. The rate of propagation dc/dn, where n is the number of cycles, was calculated as the gross mean value between the start and the end of the experiment (when one of the cords was completely detached from the matrix) and plotted against the tearing energy.

Each experimental point is the characteristic life for the total number of cycles to failure N, calculated by the Weibull statistic in a set of 6 to 10 test specimens cycled under the same amplitude. Fig. 5 shows the results for group B. It is apparent that there is a critical tearing energy under which propagation occurs, if it does, at a very slow speed. For the higher tearing energies in the limited range explored, the dependence seems to be linear, with the uncertainty given by the dispersion of the results. Extrapolation to the origin gives a critical tearing energy $\alpha_0 = 0.45\,\mathrm{kJ\,m^{-2}}$ with $K = 5.33 \times 10^{-9}\,\mathrm{m^3\,kJ}$ cycle.

In an independent experiment with tensile test pieces with a central crack, Fig. 6(a), the critical tearing energy gave the value $\alpha_0 = 0.56\,\mathrm{kJ\,m^{-2}}$ (Fig. 6b). This coincidence could be predicted taking in account that the propagation in the TCAT specimens occurs almost strictly through the rubber matrix (longitudinal cohesive fracture). From another point of view, it can be considered to be a confirmation of the value of the tearing energy for characterizing the fracture properties of the material and the independence in respect to the test specimen geometry.

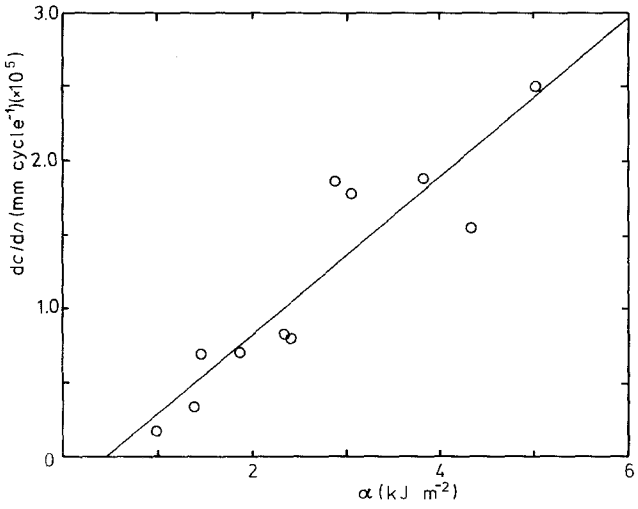

Figure 5 Variation of the crack growth rate, dc/dn, with the tearing energy in the TCAT test probe. Batch B, temperature = 40° C.

The curve obtained for a given compound at given curing conditions corresponds to the maximum adhesion strength attainable for them. Any weakening (due for example to ageing) of the adhesion interface, and the presence of partial propagation through it, would show a higher crack growth rate. This could give the basis for a test method aimed at evaluating the strength retention. This evaluation should be done at tearing energy values encountered in practice.

The results for groups A and C (Fig. 7), with much less populated experimental points, are not completely separable from those of group B. However, there seems to be some tendency indicating that the higher the temperature, the lower the crack propagation slope, with much uncertainty about critical tearing energy values. For a good discrimination, many more experiments remain to be done.

5. Discussion and conclusions

This study shows the possibility of using the TCAT test specimen in the fatigue mode to characterize the adhesion strength between steel cord and a vulcanized rubber matrix in terms of known tearing energies amplitudes or estimated stress concentration at the edge of the detached region.

Three distinct modes of failure have been observed: through the metal–rubber interface (adhesion failure), and two cohesive forms: transverse and longitudinal in respect to the wire. When adhesion is good, one of

TABLE I Compound formulation

Component	pH rubber
NR	100
HAF	63
ZnO	6
S	5
Aromatic coil	4
Antioxidant	3
Stearic acid	1
Accelerator	1

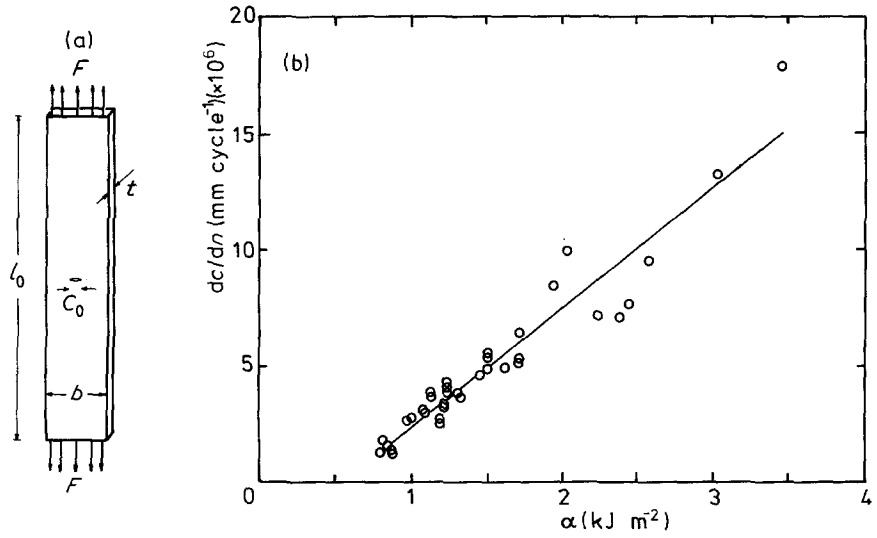

Figure 6 (a) Dimensions of the central crack test probe. l_0 = 110 mm, b = 18 mm, (b) Variation of the crack growth rate, dc/dn, with the tearing energy in the central crack test probe.

the two cohesive modes should occur. In fatigue test however, it seems the longitudinal path is the common one. A characteristic curve for the rate of propagation shows that there is a threshold tearing energy under which no propagation exists, or if it does, it should occur at very low rates. For tearing energies higher than that, the increment is linear in the range explored, even taking into account the experimental indetermination.

Then for a given compound there should be an optimum curing specification under which conditions the compound will show up its adhesion–fatigue properties. A change in the curing cycle (temperature or time) or ingredients in the formulation should be reflected in the characteristic curve or in the fatigue life. In particular, limits for the fluctuations of these parameters can be established based upon this test method, in order to prevent a weakening in the properties of either the interface or in the rubber. The onset of adhesion can be thus established, giving an important information for both the specification of the formulation and its adhesion process.

As it has been mentioned, the transverse cohesive mode is not likely to occur. The first and the last will appear as pure or combined modes, depending upon the characteristics of the cord coating, rubber matrix compound and cure conditions [12]. With modern technologies (particularly in compounding), the longitudinal cohesive is the dominant mode, thus it is worthwhile comparing the crack growth rate plotted as opposed to tearing energy in TCAT with that obtained with other test pieces commonly used [13]. A coincidence exists in the sense that a critical value of tearing energy α_0 was found that compares well with the correspondent to the central crack tensile test pieces for the same compound. However, despite the linear increase of the rate of creation of free surface area for $\alpha > \alpha_0$, the slopes are not coincident. This can be analysed from two points of view. First, the Griffith criterion, in which the tearing energy should be a universal parameter characterizing the fracture properties of the rubber matrix. In the case of the TCAT test piece, the balance of energy will not be affected by the small amount spent in rubber to steel cord friction in the detached region during the deformation cycle. However, this approach does not explain the difference in slope. Second, from the micromechanics standpoint, the stress–strain concentration should be different in TCAT when fracture has propagated, to that of conventional test pieces. For example, in TCAT those local fields must be strongly influenced by the presence of the frictional forces just behind the front of the fracture, and consequently the efficiency of the mechanism of propagation should be affected.

Taking these considerations into account, the TCAT test piece can be useful to evaluate different compounds and to optimize the curing process with respect to the temperature–time cycle, as well as studying the tolerance limits for them in order to obtain a pure cohesive mode of the fracture.

TABLE II Cure condition and modulus for the tested batches

Batch	Temperature (°C)	Modulus (MPa)
A	130	11.4
B	155	11.9
C	165	14.2

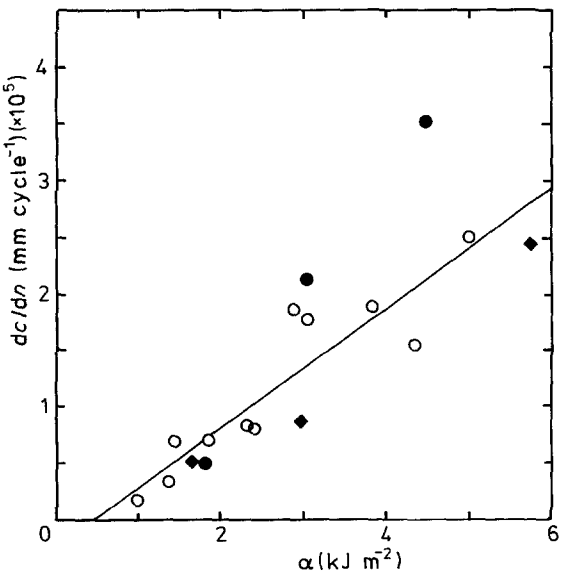

Figure 7 Comparison between different batches (●, A; ○, B; ◆, C) of the variation of dc/dn with the tearing energy.

The crack growth characteristics of the compound itself can be evaluated by means of other types of test pieces like the tensile with central or lateral crack, or pure shear, combining the resulting information properly.

Acknowledgement

The authors wish to thank FATE SAICI for giving permission to publish this paper.

References

1. D-2229-73: "Standard Method of test for adhesion of vulcanizated Rubber Cord, 1980 Annual Book of ASTM Standards", Parts 37, (American Society for Testing and Materials, Philadelphia, 1980) p. 556.
2. L. C. COATES and C. LAUER, *Rubber Chem. Technol.* **43** (1972) 16.
3. S. ECCHER and C. CANEVARI, *Kaut. Gummi Kunstst.* **22** (1969) 229.
4. A. ORBAND, G. ANTHOINE and H. ROEBUCK, *ibid.* **39** (1986) 37.
5. H. LIEVENS, *ibid.* **39** (1986) 122.
6. D. W. NICHOLSON, D. I. LIVINGSTON and G. S. FIELDING-RUSSELL, *Tire Sci. Technol.* **6** (1978) 114.
7. G. S. FIELDING-RUSSELL, D. W. NICHOLSON and D. I. LIVINGSTON, *ASTM STP* **694** (American Society for Testing and Materials, Philadelphia, 1979) p. 153.
8. A. N. GENT, G. S. FIELDING-RUSSELL, D. W. NICHOLSON and D. I. LIVINGSTONE, *J. Mater. Sci.* **16** (1981) 949.
9. R. A. RIDHA, J. F. ROACH, D. E. ERICKSON and T. F. READ, *Rubber Chem. Technol.* **54** (1981) 835.
10. R. S. RIVLIN and A. G. THOMAS, *J. Polym. Sci.* **10** (1953) 291.
11. A. G. THOMAS, Proceedings NRPRA Jubilee Conference, 1964 (edited by L. Mullins, Cambridge, 1964) p. 136.
12. W. J. VAN OOIJ, *Rubber Chem. Technol.* **57** (1984) 421.
13. J. G. LAKE, "Progress of Rubber Tech.", (Applied Science Publications Ltd, London, 1983) p. 89.

Received 30 September 1987
and accepted 26 January 1988